DALTON
FULL PAPER

Co-ordination chemistry of bis(ferrocenylcarbaldimine) Schiff bases

Peiyi Li,[a] Ian J. Scowen,[b] John E. Davies[a] and Malcolm A. Halcrow*†[a]

[a] *Department of Chemistry, University of Cambridge, Lensfield Road, Cambridge, UK CB2 1EW*
[b] *Department of Chemistry and Chemical Technology, University of Bradford, Bradford, UK BD7 1DP*

Received 25th August 1998, Accepted 2nd October 1998

The complex chemistries of 1,2-bis(ferrocen-1-ylmethyleneamino)ethane (L^1), 1,2-bis(ferrocen-1-ylmethyleneamino)benzene (L^2) and its 4-methyl (L^3), 4-chloro (L^4) and 4-nitro (L^5) derivatives have been reexamined. Complexation of L^1 by $ZnCl_2$ afforded $[ZnCl_2(L^1)]$, whose single crystal structure reveals a distorted tetrahedral zinc(II) centre with Zn · · · Fe 4.730(2) and 4.803(2) Å. The complexes $[ZnCl_2(L)]$ (L = L^2–L^5), $[ZnBr_2(L)]$ (L = L^2–L^5) and $[CoBr_2(L^3)]$ are accessible by MX_2-templated condensation of 2 equivalents of ferrocenecarbaldehyde (fcCHO) with the appropriate 1,2-diaminobenzene. Treatment of $[Cu(NCMe)_4]X$ (X^- = BF_4^- or PF_6^-) with L^1, or fcCHO and the corresponding 1,2-diaminobenzene, yielded $[Cu(L)_2]X$ (L = L^1–L^3). The single crystal structure of $[Cu(L^3)_2]$-PF_6·1.7CH_2Cl_2 shows a tetrahedral copper(I) centre, the chelate ligands being substantially distorted from planarity. Compounds $[ZnCl_2(L)]$, $[ZnBr_2(L)]$ (L = L^2–L^5) and $[CoBr_2(L^3)]$ exhibit weak electronic communication between the two ferrocenyl centres, showing by cyclic voltammetry two chemically reversible Fe^{II}–Fe^{III} oxidations separated by 50–60 mV in CH_2Cl_2–0.5 M $NBu^n_4PF_6$ at 293 K; $[ZnCl_2(L^1)]$ and $[Cu(L)_2]X$ (L = L^1–L^3) exhibit a single Fe^{II}–Fe^{III} couple under these conditions. Attempted template syntheses of L^2–L^5 employing other MX_2 (M = Mn, Co, Ni or Cu; X^- = Cl^-, Br^-, NO_3^-, BF_4^- or ClO_4^-) salts yielded primarily 2-ferrocenylbenzimidazole intramolecular cyclisation derivatives; the crystal structure of one such product was determined.

Introduction

Ferrocene-containing molecules are continuing to attract great interest as components in homogeneous catalysts,[1] molecular sensors,[2] and molecular magnetic[3] and non-linear optical[4] materials. Several groups have exploited Schiff base condensation of ferrocenecarbaldehyde [Fe(η-C_5H_5)(η-C_5H_4CHO)] as a facile method of substituting a ferrocene group onto an organic residue, and have studied the resultant Schiff bases [Fe(η-C_5H_5)(η-C_5H_4CR=NR′)] (R = H, Me or Ph; R′ = alkyl or aryl) for their non-linear optical[5] and ligating[6] properties. Some ferrocenyl di-Schiff base macrocycles derived from ferrocene-1,1′-dicarbaldehyde have also been structurally characterised.[7]

While monoferrocenyl Schiff bases appear to be relatively robust, previous attempts to prepare complexes of the bidentate diferrocenyl Schiff bases fcCH=NYN=CHfc (fc = ferrocenyl, Y = C_2H_4-1,2 L^1 or C_6H_4-1,2 L^2) have been unsuccessful. Two groups have previously reported the synthesis of L^1;[8,9] however, it was found that complexation of L^1 resulted in its spontaneous hydrolytic degradation, and it was necessary to reduce the L^1 aldimine moieties with AlH_4^- before a useful ligand was obtained. Similarly, attempts to prepare the related ligand L^2 by condensation of ferrocenecarbaldehyde with 1,2-diaminobenzene resulted in spontaneous intramolecular cyclisation of the inital di-Schiff base, forming instead the 2-ferrocenylbenzimidazole derivatives 1^H and 2^H.[10] Similar observations regarding the chemical sensitivity of the ferrocenecarbaldimine moiety have also been made by others.[11]

Given our interest in the preparation of ferrocene-substituted complexes,[12] we decided to re-examine this chemistry. We noted

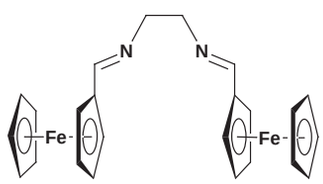

L^1

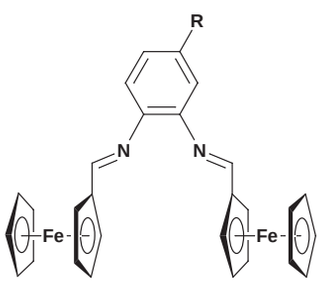

R = H; L^2
R = Me; L^3
R = Cl; L^4
R = NO_2; L^5

that (fcCH=N)$_2C_6H_4$-1,4, a geometric isomer of L^2, is stable.[13] In addition, other groups have previously reported the synthesis and complex chemistry of monoferrocenyl ligands related to L^2, of type $[fcCH{=}NC_6H_4X\text{-}2]^-$ (X^- = O^-[14] or S^-[15]). In particular, it was reported that treatment of **3**[16] with salts of Ni^{II}, Zn^{II} or Pd^{II} resulted in opening of the thiazoline ring, affording the complexes *trans*-[M(*N*,*S*-fcCH=NC_6H_4S-2)$_2$] (M = Ni, Zn or Pd).[15] We therefore suspected that complexes of L^1 and L^2 might be accessible by metal-templated condensations of fcCHO with the appropriate diamine, thus removing the

† *Current address:* School of Chemistry, University of Leeds, Woodhouse Lane, Leeds, UK LS2 9JT. E-mail: M.A.Halcrow@chemistry.leeds.ac.uk

Table 1 Analytical and selected FAB mass spectrometric data for the new compounds

Compound	Analysis (%)			
	C	H	N	*m/z* [b]
4 $[ZnCl_2(L^1)]$	48.5 (49.0)	4.1 (4.1)	4.7 (4.8)	586, 551, 452
5 $[ZnCl_2(L^2)]$	52.9 (52.8)	3.8 (3.8)	4.4 (4.4)	634, 599, 500
6 $[ZnCl_2(L^3)]$	53.7 (53.5)	4.1 (4.0)	4.5 (4.3)	648, 613, 514
7 $[ZnCl_2(L^4)]$	50.4 (50.1)	3.5 (3.5)	4.2 (4.2)	668, 633, 534
8 $[ZnCl_2(L^5)]$	49.3 (48.6)	3.4 (3.4)	6.1 (6.2)	644, 545
9 $[ZnBr_2(L^2)]$	47.0 (46.4)	3.4 (3.3)	3.8 (3.9)	643, 500
10 $[ZnBr_2(L^3)]$	46.6 (47.1)	3.5 (3.5)	3.7 (3.8)	736, 657, 517
11 $[ZnBr_2(L^4)]$	44.3 (44.3)	3.0 (3.1)	3.5 (3.7)	756, 677, 534
12 $[ZnBr_2(L^5)]$	43.6 (43.7)	3.0 (3.0)	5.3 (5.5)	688, 545
13 $[CoBr_2(L^3)]$	47.1 (47.5)	3.5 (3.6)	3.6 (3.8)	731, 652, 514
14·PF_6·$2H_2O$ $[Cu(L^1)_2]PF_6·2H_2O$	50.2 (50.2)	4.4 (4.6)	4.7 (4.9)	967, 515
15·BF_4·CH_3NO_2 $[Cu(L^2)_2]BF_4·CH_3NO_2$	56.2 (56.5)	4.3 (4.2)	5.5 (5.8)	1063, 563
16·BF_4 $[Cu(L^3)_2]BF_4$	59.1 (59.1)	4.8 (4.4)	4.6 (4.8)	1091, 577
16·PF_6 $[Cu(L^3)_2]PF_6$	55.9 (56.3)	4.4 (4.2)	4.4 (4.5)	—
$[1^HH]BF_4$	57.0 (57.1)	4.3 (4.3)	4.6 (4.8)	—

[a] Calculated values in parentheses. [b] Peaks for compounds **4**–**13** are assigned to the ions $[MX_2(L)]^+$ (not always observed), $[MX(L)]^+$ and $[L]^+$ (M = ^{59}Co or ^{64}Zn; X^- = $^{35}Cl^-$ or $^{79}Br^-$; L = L^1–L^5) and exhibit the correct isotopic distributions. Peaks for **14**·BF_4–**16**·BF_4 are assigned to the ions $[^{63}Cu(L)_2]^+$ and $[^{63}Cu(L)]^+$ (L = L^1–L^3), and exhibit the correct isotopic distributions.

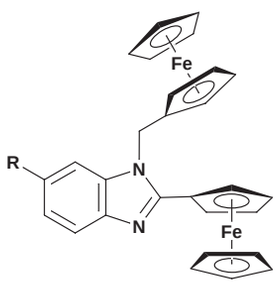

1^R (R = H, Me, Cl, NO_2)

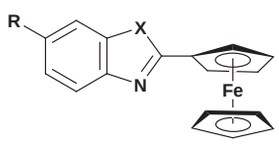

X = NH; 2^R (R = H, Me, Cl, NO_2)
X = S, R = H; 3

requirement for the free Schiff bases. We report here the results of this study.

Results and discussion

Complex syntheses

Attempted condensations of ferrocenecarbaldehyde with 1,2-diaminoethane in the presence of zinc(II) or copper(II) salts as templates afforded only en-containing complex products. We therefore decided to reinvestigate the co-ordination chemistry of preformed L^1.[8,9] As in a previous report,[9] treatment of L^1 with anhydrous MX_2 (M = Ni or Cu; X^- = Cl^- or Br^-) or hydrated $M(BF_4)_2$ (M = Ni, Cu or Zn) in CH_2Cl_2 or MeCN afforded no isolable ferrocene-containing products. However, reaction of L^1 with 1 molar equivalent of $ZnCl_2$ in CH_2Cl_2 yields large brown air-stable crystals after layering with hexanes, which analyse as $[ZnCl_2(L^1)]$ **4** (Table 1). This product is always contaminated with a small number of paler crystals of fcCHO, from which it must be separated manually. The ^{1}H and ^{13}C NMR spectra of **4** confirm that L^1 is intact in the complex, but also consistently show the presence of 10–25 mol% of fcCHO. That this contaminant originates from **4** was confirmed by ^{1}H NMR analysis of a single crystal of **4**, which clearly showed the presence of the carbaldehyde.

A large number of MX_2-templated (M = Mn, Co, Ni, Cu or Zn; X^- = Cl^-, Br^-, $MeCO_2^-$ or NO_3^-) condensations of fcCHO with 1,2-diaminobenzene, 1,2-diamino-4-methylbenzene, 1,2-diamino-4-chlorobenzene or 1,2-diamino-4-nitrobenzene were attempted, with the aim of producing complexes of stoichiometry $[MX_2(L)]$ (L = L^2–L^5). When $ZnCl_2$ or $ZnBr_2$ was used, syntheses in refluxing $CHCl_3$ gave the complexes $[ZnCl_2(L)]$ (L = L^2 **5**, L^3 **6**, L^4 **7** or L^5 **8**) and $[ZnBr_2(L)]$ (L = L^2 **9**, L^3 **10**, L^4 **11** or L^5 **12**; Table 1) in moderate yields. Similar reactions involving all these diaminobenzene derivatives with other zinc(II) salts or salts of Mn^{II}, Co^{II} or Ni^{II} yielded crude solids containing predominantly $\mathbf{1^R}$, $[\mathbf{1^R}H]X$ and/or $\mathbf{2^R}$ (R = H, Me, Cl or NO_2).[10] In only one case it was possible to purify a $[MX_2(L)]$ complex from these reactions containing a metal other than zinc, namely $[CoBr_2(L^3)]$ **13**.

Compounds **5**–**13** are all moderately soluble deep red microcrystalline solids. The ^{1}H and ^{13}C NMR spectra of **5**–**12** in $CDCl_3$ are free from fcCHO and are consistent with the presence of intact L^2–L^5 (^{13}C spectra of **8** and **12** could not be obtained because of their reduced solubility), showing that intramolecular cyclisation to $\mathbf{1^R}$ has not occurred. The paramagnetic ^{1}H NMR spectrum of **13** in $CDCl_3$ is also consistent with the presence of L^3, and was assigned from the peak integrals and by comparison with literature spectra of related complexes (Experimental section).[17] Interestingly, the ferrocenyl proton resonances exhibit upfield contact shifts, consistent with a π-spin-delocalisation pathway. This implies that substantial conjugation exists between the ferrocene and cobalt(II) centres of the complex.

In an attempt to produce complexes of formula $[M(L)_2]^{2+}$ (L = L^2–L^5), hydrated $M(BF_4)_2$ (M = Co, Ni, Cu or Zn) and $Mn(ClO_4)_2$ salts were treated with fcCHO and the appropriate diaminobenzene in a 1:4:2 mole ratio in refluxing CH_3OH. Generally, these reactions again afforded only $\mathbf{1^R}$ or $[\mathbf{1^R}H]X$. However, when M = Cu and L = L^2 or L^3, deep red products were obtained of stoichiometry $[Cu(L)_2]BF_4$ (L = L^2, **15**·BF_4 or L^3, **16**·BF_4; Table 1). Both compounds afforded diamagnetic ^{1}H NMR spectra, confirming that reduction of Cu^{II} to Cu^I had taken place. The reductant is probably fcCHO, since increased yields were obtained when excess of it was employed in these syntheses. Further improved yields of **15**·X and **16**·X (X^- = BF_4^- or PF_6^-) could be obtained by employing $[Cu(NCMe)_4]X$ rather than a copper(II) salt as template under the conditions described above. Complexation of $[Cu(NCMe)_4]PF_6$ by preformed L^1 afforded an orange product $[Cu(L^1)_2]PF_6$ **14**·PF_6. Although air-stable as solids, **14**·PF_6–**16**·BF_4 decompose in chlorinated solvents, $MeNO_2$ or MeCN over a period of days.

Table 2 Selected bond lengths (Å) and angles (°) for $[ZnCl_2(L^1)]$ **4**

Zn(1)–Cl(1)	2.223(1)	C(1)–C(2)	1.506(7)
Zn(1)–Cl(2)	2.210(1)	N(2)–C(2)	1.487(6)
Zn(1)–N(1)	2.073(4)	N(2)–C(20)	1.270(6)
Zn(1)–N(2)	2.063(3)	C(10)–C(11)	1.440(6)
N(1)–C(10)	1.281(6)	C(20)–C(21)	1.441(6)
C(1)–N(1)	1.466(6)		
Cl(1)–Zn(1)–Cl(2)	114.06(6)	C(1)–C(2)–N(2)	107.7(4)
Cl(1)–Zn(1)–N(1)	116.3(1)	C(2)–N(2)–Zn(1)	107.2(3)
Cl(1)–Zn(1)–N(2)	112.8(1)	C(20)–N(2)–Zn(1)	135.5(3)
Cl(2)–Zn(1)–N(1)	111.6(1)	C(2)–N(2)–C(20)	117.3(4)
Cl(2)–Zn(1)–N(2)	114.6(1)	N(1)–C(10)–C(11)	127.1(4)
N(1)–Zn(1)–N(2)	84.3(1)	C(10)–C(11)–C(12)	129.8(4)
C(1)–N(1)–Zn(1)	106.6(3)	C(10)–C(11)–C(15)	121.9(4)
C(10)–N(1)–Zn(1)	135.9(3)	N(2)–C(20)–C(21)	126.6(4)
C(1)–N(1)–C(10)	117.6(4)	C(20)–C(21)–C(22)	130.2(4)
N(1)–C(1)–C(2)	109.1(4)	C(20)–C(21)–C(25)	122.3(4)

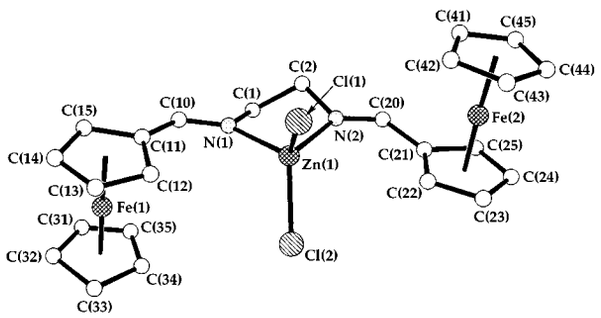

Fig. 1 Structure of the $[ZnCl_2(L^1)]$ molecule in the crystal of complex **4**, showing the atom numbering scheme employed. For clarity, all hydrogen atoms have been omitted.

Single crystal structures

A single crystal X-ray analysis of complex **4** shows the expected pseudo-tetrahedral zinc(II) centre (Fig. 1, Table 2). The Zn–Cl bond lengths are typical of those observed for such compounds; however, the Zn–N distances are somewhat short compared to other zinc(II) Schiff base complexes.[18] Aside from the acute N(1)–Zn(1)–N(2) angle of 84.3(1)° enforced by the bite of L^1, the donor atoms adopt a nearly regular tetrahedral geometry. Hence, the average bond angle at Zn(1) is 108.9°, compared to 109.5° for an 'ideal' tetrahedron, while the dihedral angle 'θ' between the planes of [Zn(1), Cl(1), Cl(2)] and [Zn(1), N(1), N(2)] is 87.3(2)°, compared to an ideal value of 90°. The ferrocenyl substituents are in a *transoid* arrangement with respect to each other and are almost coplanar with the L^1 aldimine groups, the dihedral angle between the planes [C(11)–C(15)] and [C(11)–C(10)–N(1)] being 8.7(2)° and that formed by [C(21)–C(25)] and [C(21)–C(20)–N(2)] being 8.5(2)°. This means that one α-C–H bond of each substituted C_5H_4 ring is oriented close to the zinc(II) ion, with Zn(1)···H(12) 2.90 and Zn(1)···H(22) 2.86 Å. Other bond lengths and angles within the molecule are unexceptional. The intermetallic distances are Zn(1)···Fe(1) 4.803(2), Zn(1)···Fe(2) 4.730(2) and Fe(1)···Fe(2) 9.522(2) Å.

While salts of $\mathbf{14}^+$ and $\mathbf{15}^+$ do not crystallise well, platelets of $\mathbf{16}\cdot BF_4$ and $\mathbf{16}\cdot PF_6$ could be obtained by layering concentrated CH_2Cl_2 solutions of the complexes with hexanes. Structural analyses of both salts were undertaken; unfortunately, crystals of $\mathbf{16}\cdot BF_4\cdot CH_2Cl_2$ [orthorhombic, space group *Pbca*, $a = 22.387(5)$, $b = 21.830(4)$, $c = 22.877(5)$ Å] included a second (minor) crystal domain while $\mathbf{16}\cdot PF_6\cdot 1.7CH_2Cl_2$ suffered substantial disorder of the lattice solvent. Since the complex cations in both structures were crystallographically indistinguishable, only the structure of $\mathbf{16}\cdot PF_6$ will be discussed in detail.

The structure contains one complex cation in the asymmetric unit, which exhibits a distorted tetrahedral structure with Cu–N distances of 2.030(9)–2.071(8) Å (Table 3, Fig. 2). The average N–Cu–N angle in the structure is 110.4°, while the dihedral angle 'θ' between the planes of the L^3 ligands [N(1A), Cu(1), N(2A)] and [N(1B), Cu(1), N(2B)] is 87.8(3)°. Therefore, while the geometry at copper is distorted by the bite of the L^3 chelate, there is minimal flattening of the CuN_4 tetrahedron. Other reported copper(I) complexes of diimine chelates often exhibit substantially flattened structures, with θ as low as 49°.[19,20] In contrast to **4**, the ferrocenyl substituents on each ligand are *cisoid* to each other. The Cu···Fe distances are Cu(1)···Fe(1) 4.783(2), Cu(1)···Fe(2) 5.097(3), Cu(1)···Fe(3) 4.651(2), Cu(1)···Fe(1) 5.010(2) Å, while the Fe···Fe distances range from 6.498(2) to 9.876(2) Å.

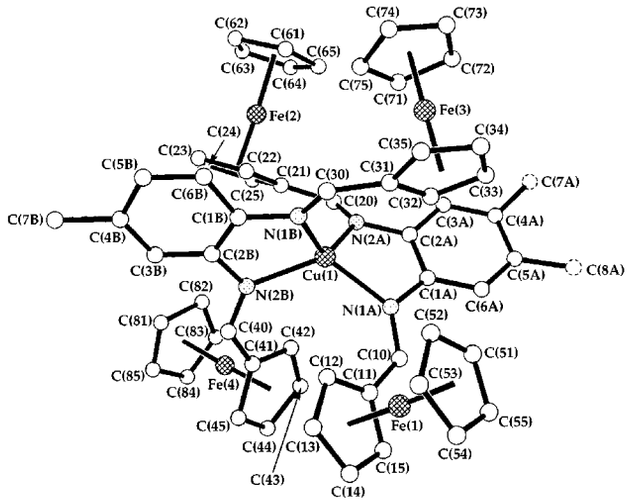

Fig. 2 Structure of the $[Cu(L^3)_2]^+$ cation in the crystal of $\mathbf{16}\cdot PF_6\cdot 1.7CH_2Cl_2$, showing the atom numbering scheme employed. For clarity, all hydrogen atoms have been omitted. The methyl substituent on one ligand is disordered over two sites C(7A) and C(8A).

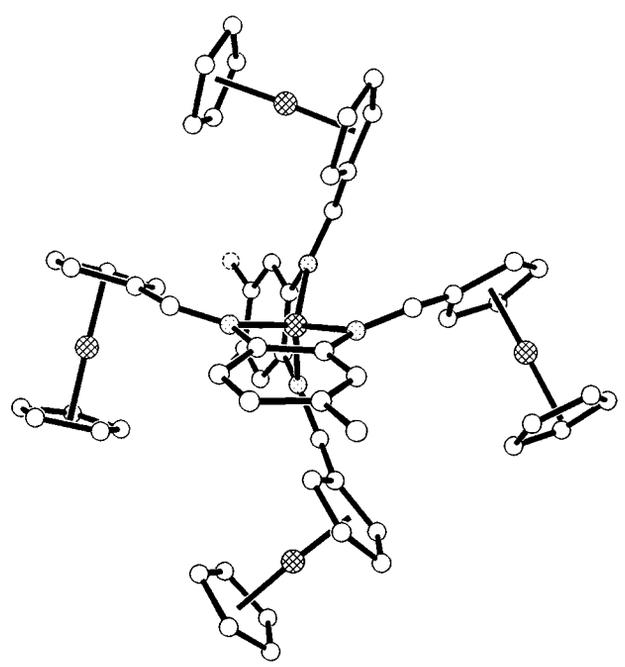

Fig. 3 Alternative view of the $[Cu(L^3)_2]^+$ cation in the crystal of $\mathbf{16}\cdot PF_6\cdot 1.7CH_2Cl_2$, emphasising the bending of the L^3 ligands. Details as for Fig. 2.

Despite the regular geometry at copper, the L^3 ligands are substantially distorted from planarity (Fig. 3). This distortion is characterised by the dihedral angles between the phenylene and ferrocenecarbaldimine moieties, and between the phenylene ring and the plane formed the two N donors and copper ion (Table 4), both of which should be zero for a planar, fully con-

Table 3 Selected bond lengths (Å) and angles (°) for $[Cu(L^3)_2]PF_6 \cdot 1.7CH_2Cl_2$ **16**$\cdot PF_6 \cdot 1.7CH_2Cl_2$

Cu(1)–N(1A)	2.071(8)	C(10)–C(11)	1.40(1)
Cu(1)–N(1B)	2.030(9)	C(20)–C(21)	1.45(1)
Cu(1)–N(2A)	2.050(8)	N(1B)–C(30)	1.30(1)
Cu(1)–N(2B)	2.041(9)	C(1B)–N(1B)	1.41(1)
N(1A)–C(10)	1.32(1)	C(1B)–C(2B)	1.38(2)
C(1A)–N(1A)	1.43(1)	N(2B)–C(2B)	1.40(1)
C(1A)–C(2A)	1.39(1)	N(2B)–C(40)	1.27(1)
N(2A)–C(2A)	1.42(1)	C(30)–C(31)	1.45(1)
N(2A)–C(20)	1.32(1)	C(40)–C(41)	1.43(2)
N(1A)–Cu(1)–N(1B)	128.7(3)	N(2A)–C(20)–C(21)	125(1)
N(1A)–Cu(1)–N(2A)	81.9(3)	C(20)–C(21)–C(22)	127(1)
N(1A)–Cu(1)–N(2B)	121.5(3)	C(20)–C(21)–C(25)	126(1)
N(1B)–Cu(1)–N(2A)	125.5(3)	C(1B)–N(1B)–Cu(1)	108.9(7)
N(1B)–Cu(1)–N(2B)	81.9(4)	C(30)–N(1B)–Cu(1)	132.1(8)
N(2A)–Cu(1)–N(2B)	123.1(3)	C(1B)–N(1B)–C(30)	119(1)
C(1A)–N(1A)–Cu(1)	107.2(6)	N(1B)–C(1B)–C(2B)	119(1)
C(10)–N(1A)–Cu(1)	132.4(7)	N(1B)–C(1B)–C(6B)	123(1)
C(1A)–N(1A)–C(10)	120.1(8)	N(2B)–C(2B)–C(1B)	116(1)
N(1A)–C(1A)–C(2A)	118.7(9)	N(2B)–C(2B)–C(3B)	123(1)
N(1A)–C(1A)–C(6A)	123.1(9)	C(2B)–N(2B)–Cu(1)	110.4(7)
N(2A)–C(2A)–C(1A)	116.1(8)	C(40)–N(2B)–Cu(1)	130.7(8)
N(2A)–C(2A)–C(3A)	123.2(9)	C(2B)–N(2B)–C(40)	117(1)
C(2A)–N(2A)–Cu(1)	109.1(6)	N(1B)–C(30)–C(31)	127(1)
C(20)–N(2A)–Cu(1)	131.5(7)	C(30)–C(31)–C(32)	128(1)
C(2A)–N(2A)–C(20)	118.1(9)	C(30)–C(31)–C(35)	124(1)
N(1A)–C(10)–C(11)	125.7(9)	N(2B)–C(40)–C(41)	126(1)
C(10)–C(11)–C(12)	129.1(9)	C(40)–C(41)–C(42)	127(1)
C(10)–C(11)–C(15)	122(1)	C(40)–C(41)–C(45)	129(1)

Table 4 Selected torsion angles (°) for $[Cu(L^3)_2]PF_6 \cdot 1.7CH_2Cl_2$ **16**$\cdot PF_6 \cdot 1.7CH_2Cl_2$, describing the structural distortions of the ligands

Ligand A	
[N(1A), N(2A), C(1A)–C(6A)]–[N(1A), C(10)–C(15)]	36.6(3)
[N(1A), N(2A), C(1A)–C(6A)]–[N(2A), C(20)–C(25)]	53.7(3)
[N(1A), N(2A), C(1A)–C(6A)]–[Cu(1), N(1A), N(2A)]	27.5(2)
Ligand B	
[N(1B), N(2B), C(1B)–C(6B)]–[N(1B), C(30)–C(35)]	24.3(4)
[N(1B), N(2B), C(1B)–C(6B)]–[N(2B), C(40)–C(45)]	48.1(4)
[N(1B), N(2B), C(1B)–C(6B)]–[Cu(1), N(1B), N(2B)]	21.4(4)

jugated ligand. These distortions are a consequence of a close contact formed by one α-C–H bond of each ferrocenyl group with Cu(1) (*cf.* **4**, see above). These distances are Cu(1)···H(12) 2.74, Cu(1)···H(22) 2.89, Cu(1)···H(32) 2.70, Cu(1)···H(42) 2.83 Å. Thus, the ferrocenyl units are forced to twist away from the copper ion and, in order to retain planarity at the sp^2 N atoms, the L^3 phenylene groups become displaced out of the CuN_2 plane.

Crystals of compound $[\mathbf{1}^{\mathbf{H}}H]BF_4$ were isolated from a crude reaction mixture of $Zn(BF_4)_2.6H_2O$, fcCHO and 1,2-diaminobenzene in MeCN. By comparison with the previously reported structure of unprotonated $\mathbf{1}^{\mathbf{H}}$,[10] the angle C(1)–N(2)–C(2) in $[\mathbf{1}^{\mathbf{H}}H]BF_4$ is significantly greater [110.7(4) *vs.* 104.3(4)°], while N(1)–C(1)–N(2) is correspondingly smaller [106.7(4) *vs.* 112.4(4)°] (Fig. 4, Table 5). All other bond lengths and angles in the complex molecules are crystallographically indistinguishable in the two structures. There is a hydrogen bond between the benzimidazolium proton and BF_4^- anion (Fig. 4), with N(2)···F(1) 2.772(6), H(2)···F(1) 2.03(3) Å and N–H···F 161(5)°.

UV/visible spectroscopy

Ferrocene exhibits two absorptions in the visible and near UV at $\nu_{max} = 22.7$ ($\varepsilon_{max} = 110$) and 30.8×10^3 cm^{-1} (49 M^{-1} cm^{-1}), assigned to spin-allowed d–d transitions.[21] Compounds L^1 and **4**–**13** also exhibit two absorptions in CH_2Cl_2 solution (Table 6). These transitions lie at lower energy for **4** compared to uncomplexed L^1, suggesting that the iron centres become less electron-rich upon co-ordination. Compared to **4**, the lower energy visible transition exhibited by **5**–**12** is red-shifted, as expected upon replacement of the *N*-alkyl substituent in **4** by an

Table 5 Selected bond lengths (Å) and angles (°) for $[\mathbf{1}^{\mathbf{H}}H]BF_4$

N(1)–C(1)	1.355(6)	C(2)–C(7)	1.389(6)
N(1)–C(7)	1.392(7)	C(2)–C(3)	1.396(8)
N(1)–C(10)	1.485(5)	C(3)–C(4)	1.380(8)
C(1)–N(2)	1.362(6)	C(4)–C(5)	1.378(8)
C(1)–C(31)	1.432(7)	C(5)–C(6)	1.372(8)
N(2)–C(2)	1.367(7)	C(6)–C(7)	1.394(7)
N(2)–H(2)	0.77(3)	C(10)–C(11)	1.507(6)
C(1)–N(1)–C(7)	109.3(4)	C(2)–C(3)–C(4)	116.9(5)
C(1)–N(1)–C(10)	125.8(5)	C(3)–C(4)–C(5)	121.1(5)
C(7)–N(1)–C(10)	124.9(4)	C(4)–C(5)–C(6)	122.9(5)
N(1)–C(1)–N(2)	106.7(4)	C(5)–C(6)–C(7)	116.6(5)
N(1)–C(1)–C(31)	130.0(4)	N(1)–C(7)–C(2)	107.0(4)
N(2)–C(1)–C(31)	123.3(4)	N(1)–C(7)–C(6)	132.0(4)
C(1)–N(2)–C(2)	110.7(4)	C(2)–C(7)–C(6)	121.0(5)
C(1)–N(2)–H(2)	121(5)	N(1)–C(10)–C(11)	110.9(4)
C(2)–N(2)–H(2)	128(5)	C(10)–C(11)–C(12)	127.3(4)
N(2)–C(2)–C(3)	132.3(4)	C(10)–C(11)–C(15)	124.4(5)
N(2)–C(2)–C(7)	106.3(4)	C(1)–C(31)–C(32)	123.4(5)
C(3)–C(2)–C(7)	121.4(5)	C(1)–C(31)–C(35)	129.6(4)

Table 6 The UV/visible spectroscopic data for the compounds (CH_2Cl_2, 293 K)

Compound	10^{-3} $\tilde{\nu}_{max}/cm^{-1}$ (ε_{max}/M^{-1} cm^{-1})
L^1	22.2 (760), 31.0 (2 500)
4	21.1 (2 200), 28.2 (3 800)
5	19.5 (7 100), 29.8 (21 600)
6	19.5 (6 600), 29.4 (21 000)
7	19.1 (7 900), 29.3 (24 200)
8	18.4 (7 900), 28.6 (23 000)
9	19.5 (6 400), 29.7 (19 400)
10	19.5 (7 600), 29.3 (22 800)
11	19.1 (8 400), 29.2 (24 700)
12	18.3 (9 300), 28.3 (23 900)
13	19.0 (7 700), 28.3 (22 200), 32.3 (sh)
14$\cdot PF_6$	22.0 (3 600), 29.0 (14 600), 36.6 (27 900)
15$\cdot BF_4$	20.1 (12 400), 27.8 (sh), 32.2 (36 300)
16$\cdot BF_4$	20.1 (12 300), 27.8 (sh), 31.8 (36 000)

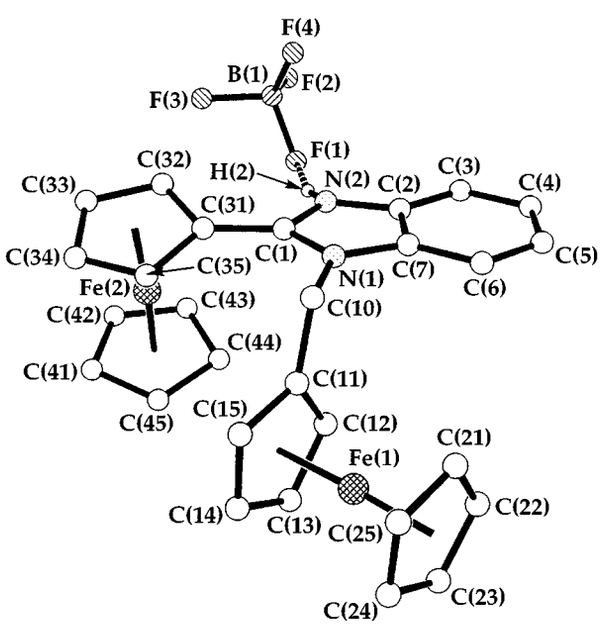

Fig. 4 Structure of the molecule in the crystal of $[\mathbf{1}^{\mathbf{H}}H]BF_4$, showing the atom numbering scheme employed. For clarity, all C-bound hydrogen atoms have been omitted.

Table 7 The UV/visible spectroscsopic data for $[ZnBr_2(L)]$ (L = L^2–L^5) in different solvents (293 K)

	Toluene	Ethyl acetate	CH_2Cl_2
E_T[a]/kcal mol^{-1}	33.9	38.1	41.1
	10^{-3} $\tilde{\nu}_{max}$/cm^{-1}		
Compound			
9	19.3, 29.3	19.6, 29.8	19.5, 29.7
10	19.3, 29.0	19.3, 29.3	19.5, 29.3
11	19.0, 28.8	19.4, 29.1	19.2, 29.2
12	18.3, 28.2	18.6, 28.7	18.3, 28.3

[a] Ref. 23.

electron-withdrawing phenylene group; anomalously, however, the higher energy near-UV absorption lies at higher energy for **5**–**12** than for **4**. For a given ligand L, the peak energies shown by $[ZnX_2(L)]$ are essentially identical for $X^- = Cl^-$ and Br^-, showing the trends in ν_{max} of $L^5 < L^4 \approx L^3 < L^2$ for the low energy band, and $L^5 < L^4 < L^3 \approx L^2$ for the higher energy peak. The intensities of these bands show small variations between compounds, however, suggesting that some solvolysis may be taking place in this solvent.

The dependence of ν_{max} on the identity of the ligand phenylene substituent suggests that the two absorption maxima shown by compounds **5**–**12** may not have pure d–d character.[22] In order to confirm this suggestion, UV/VIS spectra of **9**–**12** were run in two other weakly co-ordinating solvents, in which solvolysis of the zinc(II) centres is likely to be small. There is a small but reproducible solvatochromism associated with both UV/VIS absorptions (Table 7), which follows the polarity of the solvents as expressed by the E_T scale of Reichardt[23] reasonably well. This is behaviour expected of charge transfer rather than d–d transitions,[24] and contrasts with ferrocene whose two UV/VIS absorptions exhibit no solvatochromism.[25] Hence, it appears that both absorptions for **5**–**12** have a charge-transfer as well as (presumably) a d–d component.

The UV/VIS spectrum of compound **13** exhibits the same two absorptions as **5**–**12**, although these are red-shifted compared to **6** and **10** (Table 6). While tetrahedral cobalt(II) complexes generally show a d–d absorption in the range 15 000–20 000 cm^{-1},[24] this was not detected for **13**. Presumably, this is obscured by the stronger L^3-based absorption at 19 000 cm^{-1}. For the copper(I) complexes **14**·PF_6–**16**·BF_4, the lowest energy absorption is blue-shifted compared to those of the zinc(II) complexes of the same ligands (Table 6), consistent with the less Lewis acidic nature of the copper(I) ion. The peak near 29 000 cm^{-1} for **14**·PF_6 is also blue-shifted compared to that of **4**, and is more intense than might be expected, suggesting that this band may also contain a Cu→π* MLCT component.[19,26] For **15**·BF_4 and **16**·BF_4 this peak forms a shoulder, so that its energy and intensity cannot be accurately measured. Compounds **13**–**16**·BF_4 also exhibit an additional very intense peak above 30 000 cm^{-1}, which we assign to a Fe-based MLCT transition.[12,21]

Electrochemistry

Cyclic voltammograms of compounds **4**–**16**·BF_4 were measured in CH_2Cl_2–0.5 M $NBu^n_4PF_6$ at 293 K. All potentials are quoted *vs.* the ferrocene–ferrocenium couple, and were measured at a scan rate of 100 mV s^{-1} unless otherwise stated. The voltammetric data obtained are summarised in Table 8.

Complex **4** exhibits a single chemically reversible Fe^{II}–Fe^{III} oxidation at $E_{\frac{1}{2}} = +0.29$ V, with a peak-to-peak separation similar to that shown by ferrocene under our conditions. This half-potential for **4** is more positive than that shown by L^1 in the same solvent (+0.14 V [9]), reflecting an inductive interaction between the Lewis acidic zinc(II) ion and the L^1 iron centres. No splitting of this wave into separate one-electron components was observed [Fig. 5(a)], so that there is negligible communication between the two ferrocenyl moieties in co-ordinated L^1.

Table 8 Voltammetric data for the compounds (CH_2Cl_2–0.5 M $NBu^n_4PF_6$ or MeCN–0.1 M $NBu^n_4PF_6$, 293 K, 100 mV s^{-1}). All potentials quoted *vs.* an internal ferrocene–ferrocenium standard

Compound	Solvent	$E_{\frac{1}{2}}$ (Fe^{II}–Fe^{III})/V	Other peaks E_{p_a}/V
4	CH_2Cl_2	+0.29	—
5	CH_2Cl_2	+0.32, +0.38	—
6	CH_2Cl_2	+0.31, +0.36	—
7	CH_2Cl_2	+0.32, +0.38	—
8	CH_2Cl_2	+0.37	—
9	CH_2Cl_2	+0.32, +0.38	—
10	CH_2Cl_2	+0.31, +0.36	—
11	CH_2Cl_2	+0.33, +0.38	—
12	CH_2Cl_2	+0.36	—
13	CH_2Cl_2	+0.31, +0.37	+0.69
14·PF_6	CH_2Cl_2	+0.31[a]	+0.10[b]
	MeCN	+0.31	—
15·BF_4	CH_2Cl_2	+0.29	+0.9[c]
	MeCN	+0.30	—
16·BF_4	CH_2Cl_2	+0.27	+0.93
	MeCN	+0.23	—

[a] Irreversible process, E_{p_a} quoted. [b] Chemically reversible process, $E_{\frac{1}{2}}$ value quoted. [c] Broad peak.

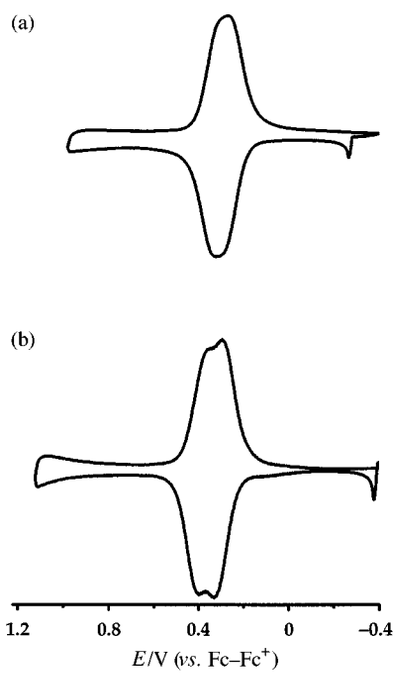

Fig. 5 Semiderivative cyclic voltammograms in CH_2Cl_2–0.5 M $NBu^n_4PF_6$ at 293 K and 100 mV s^{-1} of (a) $[ZnCl_2(L^1)]$ **4** and (b) $[ZnCl_2(L^2)]$ **5**. The irreversible ligand reduction near −1.9 V for **5** is not shown.

Importantly, this shows that electronic interactions between the iron ions in L^1 and, by extension in L^2–L^5, are not mediated by the co-ordinated zinc(II) ion. Weak communication between two ferrocenylcarbaldimine centres co-ordinated in a *trans* disposition about a nickel(II) ion has been described by others.[15,27]

In contrast to **4**, the complexes of L^2–L^4 display two distinct chemically reversible Fe^{II}–Fe^{III} oxidations at $E_{\frac{1}{2}} = +0.32 \pm 0.01$ and $+0.38 \pm 0.01$ V [Table 8; Fig. 5(b)]. The L^5 complexes **8** and **12** gave broadened cyclic voltammograms, so that no splitting of this couple could be discerned. The Fe^{II}–Fe^{III} half-potentials for the ligands in **5**–**12** follow the sequence $L^3 < L^2 \approx L^4 < L^5$, which is consistent with the inductive properties of the phenylene substituents on these ligands. For **5** and **9**, whose ferrocene substituents are in identical chemical environments, the splitting $\Delta E_{\frac{1}{2}} = 60$ mV can be taken as a measure of communication between the ferrocene centres across the phenylenediimine moiety.[28] Given the lack of a similar splitting for **4**, this electronic communication is probably mediated by the ligand π system. Complexes **6**, **7**, **10**, **11** and **13**

show an identical $\Delta E_{\frac{1}{2}}$ to those of the L^1 complexes, showing that substitution at the 4 position of the phenylene ring in L^2 affects both iron centres in the molecule to an approximately equal extent.

Complex **13** exhibits an additional irreversible oxidation with $E_{p_a} = +0.69$ V, $I_{p_a} \approx \frac{1}{2} I_{p_a}[(Fe^{II}–Fe^{III})]$ and no detectable daughter peaks, which is not exhibited by **5**–**12**. This is assigned to a $Co^{II}–Co^{III}$ process. The irreversibility of this oxidation may arise from the reduced co-ordinating ability of the 'soft' diimine ligand L^3 for a high oxidation state cobalt(III) ion, the desire of a d^6 cobalt(III) ion to attain an octahedral geometry, and/or the vulnerability of the ferrocenecarbaldimine C=N bond towards a highly Lewis acidic cobalt(III) centre.

The cyclic voltammograms of **14**·PF_6–**16**·BF_4 in CH_2Cl_2 show a single $Fe^{II}–Fe^{III}$ oxidation, whose return wave is partially obscured by a desorption spike of variable intensity, which diminishes at increased scan rates; for **14**·PF_6, this spike is particularly intense, so that the oxidation is effectively irreversible. We ascribe this behaviour to deposition of the very highly charged $[Cu(L)_2]^{n+}$ [L = L^1; $n = 6$ (see below); L = L^2 or L^3; $n = 5$] oxidation products onto the electrode, reflecting their insolubility in the non-polar CH_2Cl_2 medium. Consistent with this, cyclic voltammograms of **14**·PF_6–**16**·BF_4 in the more polar solvent MeCN–0.1 M $NBu^n_4PF_6$ now show a single chemically reversible $Fe^{II}–Fe^{III}$ oxidation (Table 8). The trend in $E_{\frac{1}{2}}(Fe^{II}–Fe^{III})$ for these complexes is **16**·BF_4 < **15**·BF_4 < **14**·PF_6, which contrasts with the behaviour observed for the $[ZnCl_2(L)]$ complexes of the same ligands, namely **4** < **6** < **5** (Table 7). The lack of communication between the ferrocenyl groups in **15**·BF_4 and **16**·BF_4 may reflect reduced conjugation within the ligands caused by twisting of the carbaldimine moieties upon coordination (Fig. 3).

The copper(I) complexes also exhibit a second oxidation, with I_{p_a} *ca.* $\frac{1}{4} I_{p_a}(Fe^{II}–Fe^{III})$. For **14**·$PF_6$ this is a chemically reversible process in CH_2Cl_2 with $E_{\frac{1}{2}} = +0.10$ V, which we assign to a $Cu^{I}–Cu^{II}$ couple. This is typical behaviour for copper(I) bis(diimine) complexes, which generally exhibit chemically reversible $Cu^{I}–Cu^{II}$ couples in the range $E_{\frac{1}{2}} = –0.3$ to 0.7 V.[19,29] In MeCN this peak is not observed, and is probably obscured by the $Fe^{II}–Fe^{III}$ oxidation. Since $E_{\frac{1}{2}}(Cu^{I}–Cu^{II}) < E_{\frac{1}{2}}(Fe^{II}–Fe^{III})$ in CH_2Cl_2, the $Fe^{II}–Fe^{III}$ half-potential measured for **14**·PF_6 in this solvent is in fact derived from the species $[Cu(L^1)_2]^{2+}$. This probably explains the increased $E_{p_a}(Fe^{II}–Fe^{III})$ value measured for **14**·PF_6 compared to that for **4** (see above). For **15**·BF_4 and **16**·BF_4 a broad irreversible oxidation occurs in CH_2Cl_2 at $E_{p_a} \approx +0.9$ V. This is a very anodic potential for a $Cu^{I}–Cu^{II}$ process, however, and given its irreversibility the assignment of this peak is therefore uncertain. This peak was not detected in MeCN.

Concluding remarks

Our results have shown that, while in contrast to previous reports[9,10] complexes of L^1–L^5 can be prepared, these ligands only form isolable complexes with certain metal centres. We ascribe these observations mainly to steric factors.

It is unusual for hydrolysis of an imine like L^1 to be promoted by coordination to a metal ion, since π-back donation into the C=N π* orbital generally reduces the electrophilicity of the imine C atom.[30] However, as this work has shown, coordinated ferrocenecarbaldimines exhibit short M···H–C contacts which can lead to substantial structural distortions within the co-ordinated ligands (*cf.* **16**·PF_6, Fig. 3). We therefore suggest that for L^1 it is the introduction of steric strain within the imine linkers upon co-ordination which leads to its rapid hydrolysis in the presence of transition ions. Ligands L^2–L^5 are less sensitive to nucleophilic attack, because of conjugation between their imine moieties and the phenylene backbone. However, given their increased conformational rigidity, steric interactions may well prevent a strong complex being formed to most metal ions, so that the intramolecular cyclisation reaction undertaken by free L^2–L^5[10] will proceed readily even in the presence of a metal ion template.

It is also noteworthy that all the complexes isolated contain metal ions that favour tetrahedral co-ordination, namely Zn^{II}, Co^{II} and Cu^{I}. It is therefore likely that the steric properties of L^2–L^5 prevent the formation of tetragonal complexes, or of co-ordination numbers >4. The preponderance of zinc(II) products in this work may reflect the relatively long metal–ligand bonds formed by Zn^{II},[18] which minimise the unfavourable Zn···H–C steric contacts. For Cu^{I}, the excellent π-donor capability of this electron-rich low-valent metal ion is presumably sufficient to overcome the extremely short Cu···H–C contacts and concomitant ligand distortions observed in **14**$^+$–**16**$^+$.

Experimental

Unless stated otherwise, all manipulations were performed in air using commercial grade solvents. Ferrocenecarbaldehyde, 1,2-diaminoethane, 1,2-diaminobenzene, 1,2-diamino-4-methylbenzene and all metal salts were used as supplied. 1,2-Bis(ferrocen-1-ylmethyleneamino)ethane (L^1) was prepared by the literature method.[9] Microanalytical, FAB mass spectrometric and UV/VIS data for the complexes in this study are listed in Tables 1 and 5.

Syntheses

$[ZnCl_2(L^1)]$ 4. A mixture of L^1 (0.45 g, 1.00×10^{-3} mol) and $ZnCl_2$ (0.14 g, 1.00×10^{-3} mol) in CH_3OH (30 cm^3) was stirred at room temperature for 3 h. The resultant orange precipitate was filtered off, air-dried and recrystallised from CH_2Cl_2–Et_2O. Yield 0.39 g, 68%. NMR spectra ($CDCl_3$, 293 K): ^{1}H, δ 8.37 (s, 2 H, N=CH), 5.13 (t, J 1.8, 4 H, fc H^2 and H^5), 4.67 (t, J 1.8, 4 H, fc H^3 and H^4), 4.35 (s, 10 H, fc C_5H_5) and 3.78 (s, 4 H, CH_2); ^{13}C; δ 170.3 (N=CH), 74.3 (fc C^1), 73.7 (fc C^2 and C^5), 71.6 (fc C^3 and C^4), 70.1 (fc C_5H_5) and 59.2 (CH_2).

$[ZnCl_2(L^2)]$ 5. Ferrocenecarbaldehyde (0.43 g, 2.00×10^{-3} mol), 1,2-diaminobenzene (0.11 g, 1.00×10^{-3} mol) and $ZnCl_2$ (0.14 g, 1.00×10^{-3} mol) were refluxed in CH_3OH (30 cm^3) for 3 h, yielding a deep red solution. Concentration of the solution and addition of an excess of Et_2O yielded a dark red solid which was recrystallised from CH_2Cl_2–Et_2O. Yield 0.46 g, 72%. NMR spectra ($CDCl_3$, 293 K): ^{1}H, δ 8.84 (s, 2 H, N=CH), 7.53 (m, 2 H, Ph H^3 and H^6), 7.41 (m, 2 H, Ph H^4 and H^5), 5.31 (t, J 1.8, 4 H, fc H^2 and H^5), 4.86 (t, J 1.8, 4 H, fc H^3 and H^4) and 4.38 (s, 10 H, fc C_5H_5); ^{13}C; δ 165.5 (N=CH), 140.4 (Ph C^1 and C^2), 128.5 (Ph C^3 and C^6), 117.5 (Ph C^4 and C^5), 76.0 (fc C^1), 75.5 (fc C^2 and C^5), 72.6 (fc C^3 and C^4) and 70.3 (fc C_5H_5).

$[ZnCl_2(L^3)]$ 6. Method as for compound **5**, using 1,2-diamino-4-methylbenzene (0.12 g, 1.00×10^{-3} mol). The product formed dark red microcrystals from CH_2Cl_2–Et_2O. Yield 0.25 g, 38%. NMR spectra ($CDCl_3$, 293 K): ^{1}H; δ 8.81 (s, 1 H), 8.80 (s, 1 H, N=CH), 7.32 (m, 3 H, Ph H^3 + H^5 + H^6), 5.29 (br s, 4 H, fc H^2 and H^5), 4.82 (br s, 4 H, fc H^3 and H^4), 4.38 (s, 5 H), 4.37 (s, 5 H, fc C_5H_5) and 2.37 (s, 3 H, CH_3); ^{13}C, δ 165.3, 164.5 (N=CH), 140.0, 138.8, 138.1 (Ph C^1, C^2 and C^4), 129.3 (Ph C^5), 117.9, 117.2 (Ph C^3 and C^6), 76.0 (fc C^1), 75.3, 75.2 (fc C^2 and C^5), 72.6, 72.4 (fc C^3 and C^4), 70.3, 70.2 (fc C_5H_5) and 21.5 (CH_3).

$[ZnCl_2(L^4)]$ 7. Method as for compound **5**, using 1,2-diamino-4-chlorobenzene (0.14 g, 1.00×10^{-3} mol). The product formed a rose-red solid from CH_2Cl_2–Et_2O. Yield 0.30 g, 45%. NMR spectra ($CDCl_3$, 293 K): ^{1}H, δ 8.81 (s, 1 H), 8.77 (s, 1 H, N=CH), 7.41 (m, 3 H, Ph H^3 + H^5 + H^6), 5.33 (br s, 2 H), 5.29 (br s, 2 H, fc H^2 and H^5), 4.92 (t, J 1.8, 2 H), 4.88 (t, J 1.8, 2 H, fc H^3 and H^4), 4.41 (s, 5 H) and 4.38 (s, 5 H, fc C_5H_5); ^{13}C,

δ 166.2, 165.7 (N=CH), 141.1, 139.0 (Ph C^1 and C^2), 134.0 (Ph C^4), 128.2 (Ph C^5), 118.6, 117.5 (Ph C^3 and C^6), 76.1, 75.8 (fc C^2 and C^5), 72.8, 72.7 (fc C^3 and C^4), 70.5, 70.4 (fc C_5H_5). The peak from fc C^1 was obscured.

[$ZnCl_2(L^5)$] 8. Method as for compound **5**, using 1,2-diamino-4-nitrobenzene (0.15 g, 1.00×10^{-3} mol). The product formed a violet-red solid from CH_2Cl_2–Et_2O. Yield 0.14 g, 21%. NMR spectrum ($CDCl_3$, 293 K): ^{1}H, δ 8.94 (s, 1 H), 8.92 (s, 1 H, N=CH), 8.41 (d, *J* 2.3, 1 H, Ph H^3), 8.27 (dd, *J* 2.3 and 9.0, 1 H, Ph H^5), 7.65 (d, *J* 9.0, 1 H, Ph H^6), 5.37 (br s, 4 H, fc H^2 and H^5), 5.03 (br s, 4 H, fc H^3 and H^4), 4.45 (s, 5 H) and 4.44 (s, 5 H, fc C_5H_5).

[$ZnBr_2(L^2)$] 9. Method as for compound **5**, using $ZnBr_2$ (0.23 g, 1.00×10^{-3} mol). The product formed a deep red solid from CH_2Cl_2–Et_2O. Yield 0.47 g, 65%. NMR spectra ($CDCl_3$, 293 K): ^{1}H, δ 8.82 (s, 2 H, N=CH), 7.53 (m, 2 H, Ph H^3 and H^6), 7.43 (m, 2 H, Ph H^4 and H^5), 5.33 (t, *J* 1.9, 4 H, fc H^2 and H^5), 4.87 (t, *J* 1.9, 4 H, fc H^3 and H^4), 4.40 (s, 10 H, fc C_5H_5); ^{13}C, δ 165.5 (N=CH), 140.5 (Ph C^1 and C^2), 128.6 (Ph C^3 and C^6), 117.7 (Ph C^4 and C^5), 76.4 (fc C^1), 75.4 (fc C^2 and C^5), 73.0 (fc C^3 and C^4) and 70.0 (fc C_5H_5).

[$ZnBr_2(L^3)$] 10. Method as for compound **9**, using 1,2-diamino-4-methylbenzene (0.12 g, 1.00×10^{-3} mol). The product formed dark red microcrystals from CH_2Cl_2–Et_2O. Yield 0.30 g, 40%. NMR spectra ($CDCl_3$, 293 K): ^{1}H, δ 8.79 (s, 1 H), 8.77 (s, 1 H, N=CH), 7.42 (m, 3 H, Ph H^3 + H^5 + H^6), 5.31 (br s, 4 H, fc H^2 and H^5), 4.81 (br s, 4 H, fc H^3 and H^4), 4.38 (s, 5 H), 4.36 (s, 5 H, fc C_5H_5) and 2.43 (s, 3 H, CH_3); ^{13}C, δ 165.4, 164.5 (N=CH), 140.1, 138.8, 138.1 (Ph C^1, C^2 and C^4), 129.4 (Ph C^5), 118.1, 117.4 (Ph C^3 and C^6), 75.9 (fc C^1), 75.3, 75.2 (fc C^2 and C^5), 73.1, 73.0 (fc C^3 and C^4), 70.3, 70.2 (fc C_5H_5) and 21.5 (CH_3).

[$ZnBr_2(L^4)$] 11. Method as for compound **9**, using 1,2-diamino-4-chlorobenzene (0.14 g, 1.00×10^{-3} mol). The product formed a dark red solid from CH_2Cl_2–Et_2O. Yield 0.40 g, 53%. NMR spectra ($CDCl_3$, 293 K): ^{1}H, δ 8.82 (s, 1 H), 8.71 (s, 1 H, N=CH), 7.37 (m, 3 H, Ph H^3 + H^5 + H^6), 5.35 (br s, 2 H), 5.29 (br s, 2 H, fc H^2 and H^5), 4.90 (t, *J* 1.8, 2 H), 4.85 (t, *J* 1.8, 2 H, fc H^3 and H^4), 4.41 (s, 5 H) and 4.38 (s, 5 H, fc C_5H_5); ^{13}C, δ 166.1, 165.9 (N=CH), 141.0, 139.0 (Ph C^1 and C^2), 133.8 (Ph C^4), 128.2 (Ph C^5), 118.9, 117.6 (Ph C^3 and C^6), 76.4 (fc C^1), 75.4 (fc C^2 and C^5), 73.0 (fc C^3 and C^4) and 70.0 (fc C_5H_5).

[$ZnBr_2(L^5)$] 12. Method as for compound **9**, using 1,2-diamino-4-nitrobenzene (0.15 g, 1.00×10^{-3} mol). The product formed a violet-red solid from CH_2Cl_2–Et_2O. Yield 0.30 g, 39%. NMR spectrum ($CDCl_3$, 293 K): ^{1}H, δ 8.91 (s, 1 H), 8.89 (s, 1 H, N=CH), 8.40 (d, *J* 2.3, 1 H, Ph H^3), 8.27 (dd, *J* 2.3 and 9.0, 1 H, Ph H^5), 7.65 (d, *J* 9.0, 1 H, Ph H^6), 5.39 (br s, 4 H, fc H^2 and H^5), 5.03 (br s, 4 H, fc H^3 and H^4), 4.46 (s, 5 H) and 4.45 (s, 5 H, fc C_5H_5).

[$CoBr_2(L^3)$] 13. Method as for compound **5**, using 1,2-diamino-4-methylbenzene (0.12 g, 1.00×10^{-3} mol) and $CoBr_2$ (0.22 g, 1.00×10^{-3} mol). The product formed a violet-red solid from CH_2Cl_2–Et_2O. Yield 0.25 g, 34%. NMR spectrum ($CDCl_3$, 293 K): ^{1}H, δ 19.7 (1 H, Ph H^5), 6.8 (1 H), 6.5 (1 H, Ph H^3 + H^6), 5.3 (3 H, CH_3), −1.2 (5 H), −1.3 (5 H, fc C_5H_5), −2.7 (4 H, fc H^3 and H^4) and −21.9 (v br, *ca.* 4H, fc H^2 and H^5).

[$Cu(L^1)_2$]PF_6 14·PF_6. A solution of L^1 (0.45 g, 1.00×10^{-3} mol) and [$Cu(NCCH_3)_4$]PF_6 (0.19 g, 5.00×10^{-4} mol) in CH_3OH (30 cm^3) was stirred at room temperature under N_2 for 3 h. The orange solution was filtered, then concentrated to 3 cm^3. Layering with Et_2O afforded orange microcrystals, which were recrystallised from CH_3NO_2–Et_2O. Yield 0.48 g, 86%. NMR spectra (CD_3NO_2, 293 K): ^{1}H, δ 8.37 (s, 2 H, N=CH), 5.13 (t, *J* 1.8, 4 H, fc H^2 and H^5), 4.67 (t, *J* 1.8, 4 H, fc H^3 and H^4), 4.35 (s, 10 H, fc C_5H_5), 3.78 (s, 4 H, CH_2); ^{13}C, δ 165.6 (N=CH), 79.9 (fc C^1), 74.2 (fc C^2 and C^5), 70.4 (fc C^3, C^4 and C_5H_5) and 54.9 (CH_2).

[$Cu(L^2)_2$]BF_4 15·BF_4. *Method A.* Ferrocenecarbaldehyde (0.43 g, 2.00×10^{-3} mol), 1,2-diaminobenzene (0.11 g, 1.00×10^{-3} mol) and $Cu(BF_4)_2 \cdot xH_2O$ (0.18 g, 5.00×10^{-4} mol) were refluxed in CH_3OH (30 cm^3) for 3 h, yielding a deep red solution. Concentration of the solution and addition of an excess of Et_2O yielded a dark red solid which was recrystallised from CH_3NO_2–Et_2O. Yield 0.29 g, 50%.

Method B. As for method A, using [$Cu(NCCH_3)_4$]BF_4 (0.16 g, 5.00×10^{-4} mol). Yield 0.39 g, 68%. NMR spectra ($CDCl_3$, 293 K): ^{1}H, δ 8.47 (s, 4 H, N=CH), 7.46 (m, 8 H, Ph H^3–H^6), 4.53 (t, *J* 1.8, 8 H, fc H^2 and H^5), 4.27 (t, 1.8 Hz, 8 H, fc H^3 and H^4) and 4.07 (s, 20 H, fc C_5H_5); ^{13}C, δ 161.7 (N=CH), 143.8 (Ph C^1 and C^2), 128.3 (Ph C^3 and C^6), 118.6 (Ph C^4 and C^5), 78.4 (fc C^1), 72.7 (fc C^2 and C^5), 69.8 (fc C^3 and C^4) and 69.6 (fc C_5H_5).

[$Cu(L^3)_2$]BF_4 16·BF_4. Method as for compound **15**·BF_4, using 1,2-diamino-4-methylbenzene (0.12 g, 1.00×10^{-3} mol). The product formed dark red microcrystals from CH_3NO_2–Et_2O. Yields: method A, 0.30 g, 51%; B, 0.40 g, 68%. NMR spectra ($CDCl_3$, 293 K): ^{1}H, δ 8.43 (s, 2 H), 8.41 (s, 2 H, N=CH), 7.27 (m, 6 H, Ph H^3, H^5 and H^6), 4.52 (t, *J* 2.0, 8 H, fc H^2 and H^5), 4.27 (t, *J* 2.0, 8 H, fc H^3 and H^4), 4.08 (s, 10 H), 4.06 (s, 10 H, fc C_5H_5) and 2.54 (s, 6H, CH_3); ^{13}C; δ 161.3, 160.6 (N=CH), 143.5, 141.4, 138.5 (Ph C^1, C^2 and C^4), 118.8, 118.2 (Ph C^5 and C^6), 78.4 (fc C^1), 75.5 (fc C^2 and C^5), 72.6 (fc C^3 and C^4), 70.3 (fc C_5H_5) and 21.4 (CH_3).

[$Cu(L^3)_2$]PF_6 16·PF_6. Method as for compound **16**·BF_4, using [$Cu(NCCH_3)_4$]BF_4 (0.19 g, 5.00×10^{-4} mol). Yield: 0.44 g, 74%.

Single crystal structure determinations

Single crystals of [$ZnCl_2(L^1)$] **4** and [$Cu(L^3)_2$]PF_6 **16**·PF_6 were grown from CH_2Cl_2–hexanes. Crystals of [1^HH]BF_4 were obtained by vapour diffusion of Et_2O into a MeCN solution of the crude solid obtained from the reaction of $Zn(BF_4)_2.6H_2O$, fcCHO and 1,2-diaminobenzene in MeOH; the microanalysis of this product is given in Table 1. Experimental details from the structure determinations are given in Table 9.

Intensity data for compounds **4** and [1^HH]BF_4 were collected on a Stoe IPDS diffractometer (Mo-Kα, $\lambda = 0.71073$ Å), for **16**·$PF_6 \cdot 1.7CH_2Cl_2$ on a Rigaku RAXIS IIc diffractometer (Mo-Kα, $\lambda = 0.71069$ Å). All structures were solved by direct methods [31] and refined by full matrix least squares on F^2.[32]

[$ZnCl_2(L^1)$] 4. During refinement, high thermal parameters at carbon for both $[C_5H_5]^-$ units in the molecule were suggestive of librational disorder in these groups. One of these was successfully modelled over two orientations C41–C45 and C412–C452 with a 65 : 35 occupancy ratio. After isotropic refinement of all non-H atoms, an empirical absorption correction [33] was applied to the data. In the final cycles of refinement all full occupancy non-hydrogen atoms were assigned anisotropic displacement parameters.

[$Cu(L^3)_2$]$PF_6 \cdot 1.7CH_2Cl_2$ 16·$PF_6 \cdot 1.7CH_2Cl_2$. During refinement, the methyl substituent of ligand 'A' was found to be disordered equally over two sites, C(7A) and C(8A). No disorder in the $[C_5H_5]^-$ rings or PF_6^- anion was detected. However, the CH_2Cl_2 solvent was disordered over a substantial fraction

Table 9 Experimental details for the single crystal structure determinations

	4	**16**·PF_6·1.7CH_2Cl_2	$[1^HH]BF_4$
Formula	$C_{24}H_{24}Cl_2Fe_2N_2Zn$	$C_{59.7}H_{55.4}Cl_{3.4}CuF_6Fe_4N_4P$	$C_{28}H_{25}BF_4Fe_2N_2$
M_r	588.42	1381.32	588.01
Crystal class	Orthorhombic	Monoclinic	Monoclinic
Space group	$P2_12_12_1$ (no. 19)	$P2_1/c$ (no. 14)	$P2_1/c$ (no. 14)
a/Å	11.297(2)	17.091(5)	10.966(2)
b/Å	14.614(3)	20.019(5)	15.935(3)
c/Å	14.625(3)	17.797(5)	14.829(3)
β/°	—	95.67(4)	108.45(3)
U/Å^3	2414.5(8)	6059(3)	2458.1(9)
Z	4	4	4
μ(Mo-Kα)/mm^{-1}	2.406	1.518	1.232
T/K	293(2)	180(2)	293(2)
Measured reflections	4174	12736	8511
Independent reflections	4174	7409	3770
R_{int}	—	0.112	0.074
$R(F)$	0.035	0.075	0.061
$wR(F^2)$	0.087	0.167	0.175
Goodness of fit	1.046	0.947	1.032
Flack parameter	0.00(2)	—	—

of the asymmetric unit. This was modelled using 6 different molecules with occupancies of 0.1–0.5, 3 of which showed disorder in their Cl atoms; all C–Cl distances were fixed to a common value, which refined to 1.69(2) Å. All wholly occupied non-H atoms were refined anisotropically.

$[1^HH]BF_4$. During refinement high thermal parameters at carbon for one of the $[C_5H_5]^-$ moieties in the molecule were suggestive of librational disorder in this group. This was modelled over two orientations C41–C45 and C412–C452 with a 80 : 20 occupancy ratio. After isotropic refinement of all non-H atoms, an empirical absorption correction [34] was applied to the data. In the final cycles of refinement all full occupancy non-H atoms were assigned anisotropic displacement parameters. The benzimidazolium atom H(2) was located during refinement, and allowed to refine freely. All other H atoms were placed in calculated positions.

CCDC reference number 186/1185.

See http://www.rsc.org/suppdata/dt/1998/3791/ for crystallographic files in .cif format.

Other measurements

Infrared spectra were obtained as Nujol mulls between 4000 and 400 cm^{-1} using a Perkin-Elmer Paragon 1000 spectrophotometer, UV/VIS spectra with a Perkin-Elmer Lambda 12 spectrophotometer operating between 1100 and 200 nm in 1 cm quartz cells, NMR spectra on a Bruker DPX250 spectrometer, operating at 250.1 (^{1}H) and 62.9 MHz (^{13}C) and fast atom bombardment mass spectra on a Kratos MS890 spectrometer, employing a 3-nitrobenzyl alcohol matrix. The CHN microanalyses were performed by the University of Cambridge Department of Chemistry microanalytical service. Electrochemical measurements were carried out using an Autolab PGSTAT20 voltammetric analyser, in CH_2Cl_2 or MeCN containing 0.1 or 0.5 M $NBu^n_4PF_6$, respectively, as supporting electrolyte. Voltammetric experiments involved the use of a double platinum working/counter electrode and a silver wire reference electrode; all potentials are referenced to an internal ferrocene–ferrocenium standard and were obtained at a scan rate of 100 mV s^{-1}.

Acknowledgements

The authors thank the Royal Society (M. A. H.), the Committee of Vice-Chancellors and Principles and the Cambridge Commonwealth Trust (P. L.), the University of Cambridge and St. Catharine′s College for financial support.

References

1 A. Togni and T. Hayashi (Editors), *Ferrocenes. Homogeneous Catalysis. Organic Synthesis. Materials Science*, VCH, Weinheim, 1995.
2 P. D. Beer, *Adv. Inorg. Chem.*, 1992, **39**, 79; P. D. Beer and D. K. Smith, *Prog. Inorg. Chem.*, 1997, **46**, 1.
3 J. S. Miller and A. J. Epstein, *Angew. Chem., Int. Ed. Engl.*, 1994, **33**, 385.
4 N. J. Long, *Angew. Chem., Int. Ed. Engl.*, 1995, **34**, 21; S. R. Marder, in *Inorganic Materials*, eds. D. W. Bruce and D. O'Hare, Wiley, Chichester, 1996, ch. 3, pp. 121–169.
5 A. Houlton, N. Jasim, R. M. G. Roberts, J. Silver, D. Cunningham, P. McArdle and T. Higgins, *J. Chem. Soc., Dalton Trans.*, 1992, 2235; A. Houlton, J. R. Miller, J. Silver, N. Jasim, M. J. Ahmet, T. L. Axon, D. Bloor and G. H. Gross, *Inorg. Chim. Acta*, 1993, **205**, 67; J. Silver, J. R. Miller, A. Houlton and M. J. Ahmet, *J. Chem. Soc., Dalton Trans.*, 1994, 3355; R. Bosque, C. Lopez, J. Sales, X. Solans and M. Font-Bardia, *J. Chem. Soc., Dalton Trans.*, 1994, 735; Y. J. Wu, S. Q. Huo and Y. Zhu, *J. Organomet. Chem.*, 1995, **485**, 161; S. Q. Huo and Y. J. Wu, *J. Organomet. Chem.*, 1995, **490**, 243; C. Lopez, R. Bosque, X. Solans and M. Font-Bardia, *New J. Chem.*, 1996, **20**, 1285.
6 C. Lopez, J. Sales, X. Solans and J. Reedijk, *J. Chem. Soc., Dalton Trans.*, 1992, 2321; J. Blanco, E. Gayoso, J. M. Vila, M. Gayoso, C. Maichle-Mossmer and J. Strahle, *Z. Naturforsch., Teil B*, 1993, **48**, 906; S. Q. Huo, Y. J. Wu, Y. Zhu and L. Yang, *J. Organomet. Chem.*, 1994, **470**, 17; Y. J. Wu, S. Q. Huo, Y. Zhu and L. Yang, *J. Organomet. Chem.*, 1994, **481**, 235; R. Bosque, C. Lopez, J. Sales and X. Solans, *J. Organomet. Chem.*, 1994, **483**, 61; C. Lopez, R. Bosque, X. Solans, M. Font-Bardia, D. Tramuns, G. Fern and J. Silver, *J. Chem. Soc., Dalton Trans.*, 1994, 3039; Y. Yoshida, K. Onitsuka and K. Sonogashira, *J. Organomet. Chem.*, 1996, **511**, 47.
7 M. J. L. Tendero, A. Benito, J. M. Lloris, R. Martínez-Mañez, J. Soto, J. Payá, A. J. Edwards and P. R. Raithby, *Inorg. Chim. Acta*, 1996, **247**, 139; M. J. L. Tendero, A. Benito, R. Martínez-Mañez, J. Soto, J. Payá, A. J. Edwards and P. R. Raithby, *J. Chem. Soc., Dalton Trans.*, 1996, 343.
8 E. W. Nause, M. G. Meirim and N. F. Blom, *Organometallics*, 1988, **7**, 2562.
9 A. Benito, J. Cano, R. Martínez-Máñez, J. Soto, J. Payá, F. Lloret, M. Julve, J. Faus and M. D. Marcos, *Inorg. Chem.*, 1993, **32**, 1197.
10 A. Benito, R. Martínez-Máñez, J. Payá, J. Soto, M. J. L. Tendero and E. Sinn, *J. Organomet. Chem.*, 1995, **503**, 259.
11 J. Cano, A. Benito, R. Martínez-Máñez, J. Soto, J. Payá, F. Lloret, M. Julve, M. D. Marcos and E. Sinn, *Inorg. Chim. Acta*, 1995, **231**, 45.
12 R. J. Less, J. L. M. Wicks, N. P. Chatterton, M. J. Dewey, N. L. Cromhout, M. A. Halcrow and J. E. Davies, *J. Chem. Soc., Dalton Trans.*, 1996, 4055.
13 C. Li, X. Peng and X.-Z. You, *Synth. React. Org. Metal-Org. Chem.*, 1990, **20**, 1231; C. Li, X.-Z. You, X. Peng, C.-Y. Zhao and H.-Y. Wu, *Transition Met. Chem.*, 1995, **20**, 300.
14 D. Freiesleben, K. Polborn, C. Robl, K. Sünkel and W. Beck, *Can. J. Chem.*, 1995, **73**, 1164.

15 T. Kawamoto and Y. Kushi, *J. Chem. Soc.*, *Dalton Trans.*, 1992, 3137; I. Nagasawa, T. Kawamoto, H. Kuma and Y. Kushi, *Bull. Chem. Soc. Jpn.*, 1998, **71**, 1337.
16 P. J. Palmer, R. B. Trigg and J. V. Warrington, *J. Med. Chem.*, 1971, **14**, 248.
17 R. H. Holm, A. Chakravorty and G. O. Dudek, *J. Am. Chem. Soc.*, 1964, **86**, 379.
18 A. G. Orpen, L. Brammer, F. H. Allen, O. Kennard, D. G. Watson and R. Taylor, *J. Chem. Soc.*, *Dalton Trans.*, 1989, S1.
19 E. Müller, C. Piguet, G. Bernardinelli and A. F. Williams, *Inorg. Chem.*, 1988, **27**, 849; D. A. Bardwell, A. M. W. Cargill Thompson, J. C. Jeffrey, E. E. M. Tilley and M. D. Ward, *J. Chem. Soc.*, *Dalton Trans.*, 1995, 835; S. M. Scott, K. C. Gordon and A. K. Burrell, *Inorg. Chem.*, 1996, **35**, 2452.
20 M. A. Halcrow, N. L. Cromhout and P. R. Raithby, *Polyhedron*, 1997, **16**, 4257 and refs. therein.
21 Y. S. Sohn, D. N. Hendrickson and H. B. Gray, *J. Am. Chem. Soc.*, 1971, **93**, 3603.
22 S. Toma, A. Gáplovsky, M. Hudecek and Z. Langfelderová, *Monatsh. Chem.*, 1985, **116**, 357; M. M. Bhadbhade, A. Das, J. C. Jeffrey, J. A. McCleverty, J. A. Navas Badiola and M. D. Ward, *J. Chem. Soc.*, *Dalton Trans.*, 1995, 2769.
23 C. Reichardt, *Angew. Chem.*, *Int. Ed. Engl.*, 1965, **4**, 29.
24 A. B. P. Lever, *Inorganic Electronic Spectroscopy*, 2nd edn., Elsevier, Amsterdam, 1984.
25 D. R. Scott and R. S. Becker, *J. Chem. Phys.*, 1961, **35**, 516.
26 S. Kitagawa and M. Munakata, *Inorg. Chem.*, 1981, **20**, 2261; M. A. Masood and P. S. Zacharias, *J. Chem. Soc.*, *Dalton Trans.*, 1991, 111.
27 Z. Yu, Y. Zhou, W. Yang, Y. Tian, C.-Y. Duan, R. Liu and X. You, *Chem. Lett.*, 1996, 957.
28 M. D. Ward, *Chem. Soc. Rev.*, 1995, **24**, 121.
29 P. Federlin, J.-M. Kern, A. Rastegar, C. Dietrich-Buchecker, P. A. Marnot and J.-P. Sauvage, *New J. Chem.*, 1980, **14**, 9.
30 E. C. Constable, *Metals and Ligand Reactivity*, 2nd edn., VCH, Weinheim, 1996.
31 G. M. Sheldrick, SHELXTL PLUS, PC version, Siemens Analytical X-Ray Instruments Inc., Madison, WI, 1990.
32 G. M. Sheldrick, SHELXL 97, University of Göttingen, 1997.
33 S. Parkin, B. Moezzi and H. Hope, *J. Appl. Crystallogr.*, 1995, **28**, 53.
34 N. Walker and D. Stuart, *Acta Crystallogr.*, *Sect. A*, 1983, **39**, 158.

Paper 8/06657D